Progress In Electromagnetics Research Letters, Vol. 2, 11–20, 2008

RADIATION OF A HERTZIAN DIPOLE IN A SHORT-ENDED CONDUCTING CIRCULAR CYLINDER WITH NARROW CIRCUMFERENTIAL SLOTS

J. S. Ock and H. J. Eom

Division of Electrical Engineering and
Radiowave Detection Research Center
Korea Advanced Institute of Science and Technology
373-1 Guseong-dong, Yuseong-gu, Daejeon 305-701, Korea

Abstract—Radiation of a Hertzian dipole in a short-ended conducting circular cylinder with narrow circumferential slots is presented. Mode-matching and Fourier transform were utilized to derive a system of simultaneous equations for modal coefficients. Computations were performed to confirm the fast convergence of the series solution.

1. INTRODUCTION

Circumferentially slotted conducting circular cylinders have many important applications in slot array antennas and EMI/EMC areas. Scattering and radiation from circumferentially slotted circular cylinders, excited by TE and TM modes, were considered in [1–4] using different approaches. Hertzian-dipole radiation and scattering from a circumferentially slotted circular cylinder of infinite length were studied in [5, 6] using mode-matching and Fourier-transform. The mode-matching and other similar analysis techniques were used to analyze scattering from various slots on circular cylindrical structures [7–9]. The Green's function of magnetic current on a circular cylindrical metal surface was considered in [10]. A short-ended, circumferentially slotted circular cylinder of infinite length is also an important structure for slotted array antenna applications. The purpose of the present paper is to investigate radiation from a short-ended, perfectly conducting circular cylinder with narrow circumferential slots excited by a Hertzian dipole. The theoretical approach in this paper is similar to that in [5], which dealt with a circumferentially slotted conducting cylinder of infinite length. Fourier transform and mode-matching techniques will be utilized to develop a numerically efficient series solution.

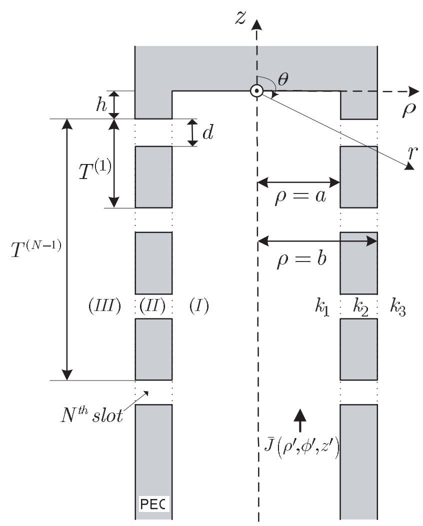

Figure 1. Geometry of problem. inner and outer radii: a and b, number of slots: N, width of the slot: d, distance from the top of q-th slot to the top of 1st slot: $T^{(q-1)}$, wave numbers of regions (I), (II), and (III): $k_1 = \omega\sqrt{\mu_1\epsilon_1}$, $k_2 = \omega\sqrt{\mu_2\epsilon_2}$ and $k_3 = \omega\sqrt{\mu_3\epsilon_3}$.

2. THEORY

Figure 1 illustrates a Hertzian dipole placed within a short-ended hollow conducting (PEC) circular cylinder with multiple narrow circumferential slots. We use the cylindrical coordinates (ρ, ϕ, z) in the analysis. The length of the cylinder is infinite in the z-direction. Note that the cylinder is short-ended at $z = 0$ and the cylindrical region above the shorted end ($0 < \rho < b$ and $z > 0$) is composed of a PEC. Regions (I), (II), and (III) denote a circular cylinder interior ($0 < \rho < a$), slotted apertures ($a < \rho < b$ and $-T^{(q)} - h - d < z < -T^{(q)} - h$), and an ambient medium ($\rho > b$), respectively. The Hertzian dipole in region (I) is given by $\bar{J} = \hat{z}\frac{J}{\rho}\delta(\rho - \rho')\,\delta(\phi - \phi')\,\delta(z - z')$ where $\delta(\cdot)$ is the Dirac delta function. The time convention $e^{-i\omega t}$ is suppressed throughout the analysis. The field in region (I) is composed of the incident and scattered fields. The current density $\bar{J}$ in a short-ended, perfectly conducting cylinder yields the z-component of incident magnetic vector potential

$$A_z^i(\rho,\phi,z;\rho',\phi',z') = \frac{\mu J}{2\pi i}\int_0^\infty \sum_{n=-\infty}^{\infty}$$
$$\left\{\begin{array}{l} \dfrac{\Omega_n(\kappa_1\rho')\,J_n(\kappa_1\rho)}{J_n(\kappa_1 a)} e^{-in(\phi-\phi')}\cos\zeta z\cos\zeta z' d\zeta,\, \rho<\rho' \\ \dfrac{J_n(\kappa_1\rho')\,\Omega_n(\kappa_1\rho)}{J_n(\kappa_1 a)} e^{-in(\phi-\phi')}\cos\zeta z\cos\zeta z' d\zeta,\, \rho>\rho' \end{array}\right. \tag{1}$$

where $\Omega_n(\kappa_1\rho) = J_n(\kappa_1\rho)H_n^{(1)}(\kappa_1 a) - H_n^{(1)}(\kappa_1\rho)J_n(\kappa_1 a)$, $\kappa_1 = \sqrt{k_1^2-\zeta^2}$, and $J_n(\cdot)$ and $H_n^{(1)}(\cdot)$ represent the nth-order Bessel and Hankel functions of the first kind, respectively. The scattered magnetic and electric vector potentials in regions (I) and (III) are

$$A_z^I(\rho,\phi,z) = \frac{2}{\pi}\sum_{n=-\infty}^{\infty} e^{-in\phi}\int_0^\infty \tilde{A}_z^I(\zeta)J_n(\kappa_1\rho)\cos\zeta z d\zeta \tag{2}$$

$$F_z^I(\rho,\phi,z) = \frac{2}{\pi}\sum_{n=-\infty}^{\infty} e^{-in\phi}\int_0^\infty \tilde{F}_z^I(\zeta)J_n(\kappa_1\rho)\sin\zeta z d\zeta \tag{3}$$

$$A_z^{III}(\rho,\phi,z) = \frac{1}{2\pi}\sum_{n=-\infty}^{\infty} e^{-in\phi}\int_{-\infty}^\infty \tilde{A}_z^{III}(\zeta)H_n^{(1)}(\kappa_3\rho)e^{-i\zeta z}d\zeta \tag{4}$$

$$F_z^{III}(\rho,\phi,z) = \frac{1}{2\pi}\sum_{n=-\infty}^{\infty} e^{-in\phi}\int_{-\infty}^\infty \tilde{F}_z^{III}(\zeta)H_n^{(1)}(\kappa_3\rho)e^{-i\zeta z}d\zeta \tag{5}$$

where $\kappa_3 = \sqrt{k_3^2-\zeta^2}$. We assume that the electric field within the narrow slots has approximately an E_z component. Thus, the electric vector potential is zero and the magnetic vector potential in region (II) is

$$A_z^{II}(\rho,\phi) = \sum_{n=-\infty}^{\infty} R_n^{(q)}(k_2\rho)e^{-in\phi} \tag{6}$$

where $R_n^{(q)}(k_2\rho) = A_n^{(q)}\dfrac{J_n(k_2\rho)}{J_n(k_2 a)} + B_n^{(q)}\dfrac{N_n(k_2\rho)}{N_n(k_2 b)}$ and $N_n(\cdot)$ is the nth-order Bessel function of the second kind. It is necessary to enforce the boundary conditions to find the coefficients $A_n^{(q)}$ and $B_n^{(q)}$. Following the method based on mode-matching and Fourier cosine transform in [5] and [11], the tangential field (E_z, E_ϕ, H_ϕ) continuities at $\rho = a$

yield

$$\sum_{q=0}^{N-1} A_n^{(q)} \left[\frac{dk_2}{\mu_2} \frac{J_n'(k_2 a)}{J_n(k_2 a)} \delta_{ql} + \frac{2n^2 I_1^{n(q,l)}}{\pi \mu_1 a^2} - \frac{2\omega^2 \varepsilon_1 I_2^{n(q,l)}}{\pi} \right] +$$

$$\sum_{q=0}^{N-1} B_n^{(q)} \left[\frac{dk_2}{\mu_2} \frac{N_n'(k_2 a)}{N_n(k_2 b)} \delta_{ql} + \frac{2n^2 I_1^{n(q,l)}}{\pi \mu_1 a^2} \frac{N_n(k_2 a)}{N_n(k_2 b)} \right.$$

$$\left. - \frac{2\omega^2 \varepsilon_1 I_2^{n(q,l)}}{\pi} \frac{N_n(k_2 a)}{N_n(k_2 b)} \right] = \frac{J e^{in\phi'}}{2\pi i} I_s^{n(l)} \tag{7}$$

where δ_{ql} is the Kronecker delta. Here the symbols $J_n'(k_2 a)$ and $N_n'(k_2 a)$ denote differentiation $dJ_n(k_2\rho)/d(k_2\rho)\big|_{\rho=a}$ and $dN_n(k_2\rho)/d(k_2\rho)\big|_{\rho=a}$, respectively, and

$$I_s^{n(l)} = \int_0^\infty \frac{\kappa_1 J_n(\kappa_1 \rho') \, \Omega_n'(\kappa_1 a)}{J_n(\kappa_1 a)} M^{(l)}(\zeta) \cos \zeta z' d\zeta \tag{8}$$

$$I_1^{n(q,l)} = \int_0^\infty \frac{\zeta^2 J_n(\kappa_1 a)}{\kappa_1^3 J_n'(\kappa_1 a)} M^{(q)}(\zeta) M^{(l)}(\zeta) d\zeta \tag{9}$$

$$I_2^{n(q,l)} = \int_0^\infty \frac{J_n'(\kappa_1 a)}{\kappa_1 J_n(\kappa_1 a)} M^{(q)}(\zeta) M^{(l)}(\zeta) d\zeta \tag{10}$$

$$M^{(q)}(\zeta) = \frac{\sin \zeta \left[T^{(q)} + d + h\right] - \sin \zeta \left[T^{(q)} + h\right]}{\zeta} \tag{11}$$

$$\Omega_n'(\kappa_1 a) = J_n'(\kappa_1 a) H_n^{(1)}(\kappa_1 a) - H_n^{(1)'}(\kappa_1 a) J_n(\kappa_1 a) \tag{12}$$

The integrals (8) $\sim$ (10) can be changed into fast convergent series on the basis of residue calculus, and results are summarized in Appendix A. The remaining boundary conditions of the tangential field continuities at $\rho = b$ yield another set of equations, which are identical with (13) in [5]. The unknown coefficients $A_n^{(q)}$ and $B_n^{(q)}$ can be determined by solving simultaneously (7) in this paper and (13) in [5]. The far-field expressions in series of $A_n^{(q)}$ and $B_n^{(q)}$ are available in [5].

3. COMPUTATIONS

To check the accuracy of the formulation, we compare our results with the results of commercially available software CST MWS [12]. We assume that N slots are uniformly distributed with a period

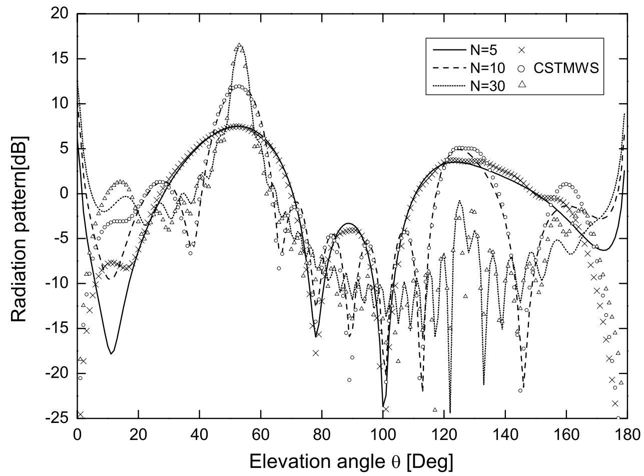

Figure 2. Angular radiation pattern as a function of slot number N: $a = 0.5\lambda$, $b = 0.6\lambda$, $d = 0.1\lambda$, $T = 0.5\lambda$, $h = 0$, $\epsilon_1 = \epsilon_2 = \epsilon_3 = \epsilon_0$, $\mu_1 = \mu_2 = \mu_3 = \mu_0$, λ: wavelength.

T $(= T^{(q)} - T^{(q-1)})$. Figure 2 illustrates the radiation pattern against the elevation angle θ at $\phi = 0$ degree when the Hertzian dipole source is located at the center ($\rho' = 0$) of a cylinder. The far field has a dominant E_θ component. An increase in the slot number N results in a sharpening of the beamwidth. The radiation efficiency for $N = 30$ is 52%. Good agreement is observed between our computed results and the results of CST MWS except for near $\theta = 0$ and 180 degrees. The discrepancies near $\theta = 0$ and 180 degrees are due to the different assumption of cylinder length. Note that CST MWS simulation uses a cylinder of finite length whereas our model uses a cylinder of infinite length. The number of modes used in our computation is one ($n = 0$), indicating good numerical efficiency. Figures 3(a) and (b) show the radiation patterns against the elevation angle θ and the azimuth angle ϕ, respectively, when the Hertzian dipole source is located off the center ($\rho' = 0.4\lambda$) of the cylinder. Good agreement with the CST MWS results is seen in Figures 3(a) and (b) where seven modes ($n = 0, \pm 1, \pm 2, \pm 3$) are used in our computation. In order to further investigate the effect of source location, the dipole source was moved closer to the slot ($\rho' = 0.56\lambda$) and the radiation patterns are shown in Figures 4(a) and (b). Our results start to deviate from the CST MWS results, particularly in Figure 4(b). The discrepancies between ours and the CST MWS result may be due to the approximation that was used to represent the electric fields within the narrow slots.

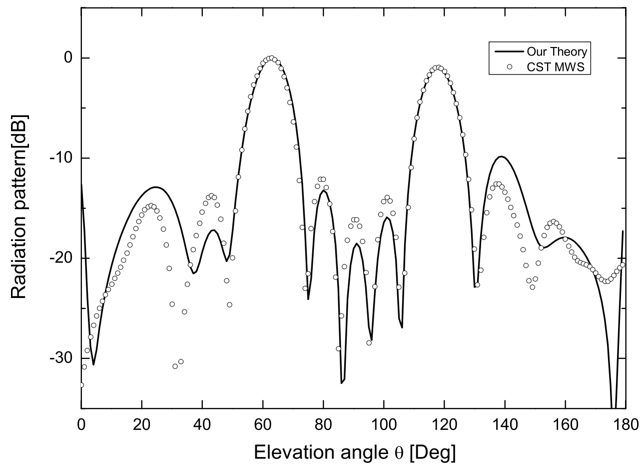

(a)

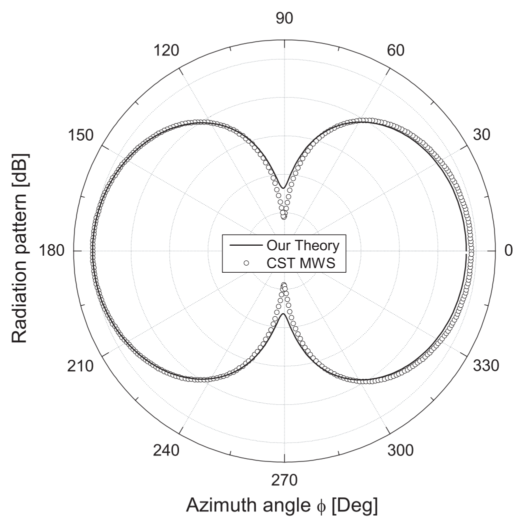

(b)

Figure 3. (a) Radiation pattern against the elevation angle θ at $\phi = 0°$: $\rho' = 0.4\lambda$, $\phi' = 0$, $z' = -9T - 0.5d$, $a = 0.7\lambda$, $b = 0.8\lambda$, $d = 0.05\lambda$, $T = 0.5\lambda$, $N = 10$, $\epsilon_1 = \epsilon_2 = \epsilon_3 = \epsilon_0$, $\mu_1 = \mu_2 = \mu_3 = \mu_0$, (b) radiation pattern against the azimuth angle ϕ at $\theta = 64°$: $\rho' = 0.4\lambda$, $\phi' = 0$, $z' = -9T - 0.5d$, $a = 0.7\lambda$, $b = 0.8\lambda$, $d = 0.05\lambda$, $T = 0.5\lambda$, $N = 10$, $\epsilon_1 = \epsilon_2 = \epsilon_3 = \epsilon_0$, $\mu_1 = \mu_2 = \mu_3 = \mu_0$.

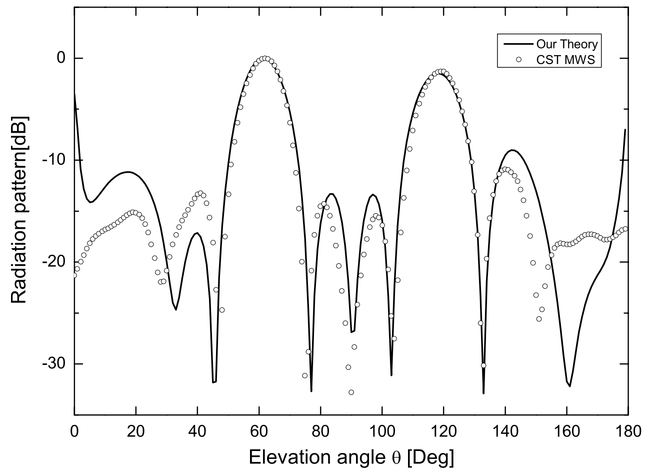

(a)

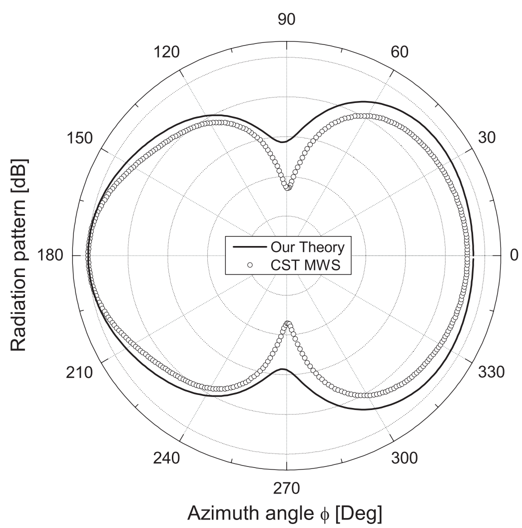

(b)

Figure 4. (a) Radiation pattern against the elevation angle θ at $\phi = 0°$: $\rho' = 0.56\lambda$, $\phi' = 0$, $z' = -9T - 0.5d$, $a = 0.7\lambda$, $b = 0.8\lambda$, $d = 0.05\lambda$, $T = 0.5\lambda$, $N = 10$, $\epsilon_1 = \epsilon_2 = \epsilon_3 = \epsilon_0$, $\mu_1 = \mu_2 = \mu_3 = \mu_0$, (b) radiation pattern against the azimuth angle ϕ at $\theta = 60°$: $\rho' = 0.56\lambda$, $\phi' = 0$, $z' = -9T - 0.5d$, $a = 0.7\lambda$, $b = 0.8\lambda$, $d = 0.05\lambda$, $T = 0.5\lambda$, $N = 10$, $\epsilon_1 = \epsilon_2 = \epsilon_3 = \epsilon_0$, $\mu_1 = \mu_2 = \mu_3 = \mu_0$.

4. CONCLUSION

A theoretical formulation for radiation from a Hertzian dipole placed in a short-ended conducting circular cylinder with narrow circumferential slots was presented. The series solution was shown to be fast convergent and numerically efficient. The presented solution is applicable to the design of short-ended circular conducting cylinders with circumferential narrow slots so long as the dipole source is not too close to the slots ($\rho'/a < 0.8$).

ACKNOWLEDGMENT

This research was supported by the Agency for Defense Development, Korea, through the Radiowave Detection Research Center at Korea Advanced Institute of Science and Technology.

APPENDIX A. SERIES REPRESENTATIONS OF INTEGRALS

$$I_s^{n(l)} = \begin{cases} \displaystyle\sum_{v=1}^{\infty} 2\Lambda_1 \cos(\zeta_v z') e^{i\zeta_v\left(T^{(l)}+h\right)} \left(e^{i\zeta_v d} - 1\right) & \text{if } z' \geq -T^{(l)} - h \\ \displaystyle\sum_{v=1}^{\infty} \Lambda_1 \Big[e^{i\zeta_v\left(T^{(l)}+h+d+z'\right)} + e^{-i\zeta_v\left(T^{(l)}+h+z'\right)} & \\ \quad + e^{i\zeta_v\left(T^{(l)}+h-z'\right)} \left(e^{i\zeta_v d} - 1\right)\Big] + \Lambda_2 & \text{if } -T^{(l)} - h - d \leq z' < -T^{(l)} - h \\ \displaystyle\sum_{v=1}^{\infty} \Lambda_1 \Big[e^{i\zeta_v\left(T^{(l)}+h-z'\right)} \left(e^{i\zeta_v d} - 1\right) & \\ \quad - e^{-i\zeta_v\left(T^{(l)}+h+z'\right)} \left(e^{-i\zeta_v d} - 1\right)\Big] & \text{if } z' < -T^{(l)} - h - d \end{cases} \tag{A1}$$

$$I_1^{n(q,l)} = \begin{cases} \displaystyle\sum_{v=1}^{\infty} \frac{\pi i a J_n(\chi'_{nv}) \mathrm{X}_1(\zeta'_v)}{2\zeta'_v (\chi'_{nv})^2 J''_n(\chi'_{nv})} + \frac{\pi i a \tau_n}{4k_1 |n|} \mathrm{X}_1(k_1) & \text{if } T^{(q)} \neq T^{(l)} \\ \displaystyle\sum_{v=1}^{\infty} \frac{\pi i a J_n(\chi'_{nv}) \mathrm{X}_2(\zeta'_v)}{2\zeta'_v (\chi'_{nv})^2 J''_n(\chi'_{nv})} + \frac{\pi i a \tau_n}{4k_1 |n|} \mathrm{X}_2(k_1) & \text{otherwise} \end{cases} \tag{A2}$$

$$I_2^{n(q,l)} = \begin{cases} \displaystyle\sum_{v=1}^{\infty} \frac{\pi i \mathrm{X}_1(\zeta_v)}{2a\zeta_v^3} + \frac{\pi i\,|n|}{4k_1^3 a}\mathrm{X}_1(k_1) & \text{if } T^{(q)} \neq T^{(l)} \\ \displaystyle\sum_{v=1}^{\infty} \frac{\pi i \mathrm{X}_2(\zeta_v)}{2a\zeta_v^3} + \frac{\pi i\,|n|}{4k_1^3 a}\mathrm{X}_2(k_1) + \frac{\pi d J_n'(k_1 a)}{2k_1 J_n(k_1 a)} & \text{otherwise} \end{cases} \tag{A3}$$

where $\tau_0 = 0$, $\tau_1 = \tau_2 = \cdots = 1$, χ_{nv} and χ'_{nv} are the zeros of the Bessel function of the first kind and its derivative, respectively, $\zeta_v = \sqrt{k_1^2 - (\chi_{nv}/a)^2}$, $\zeta'_v = \sqrt{k_1^2 - (\chi'_{nv}/a)^2}$,

$$\Lambda_1 = -\frac{\pi(\chi_{nv})^2 J_n\left(\frac{\chi_{nv}}{a}\rho'\right)\Omega_n'(\chi_{nv})}{2a^3\zeta_v^2 J_n'(\chi_{nv})} \tag{A4}$$

$$\Lambda_2 = \frac{\pi k_1 J_n(k_1\rho')\,\Omega_n'(k_1 a)}{2J_n(k_1 a)} \tag{A5}$$

$$\begin{aligned} \mathrm{X}_1(\zeta_v) &= e^{i\zeta_v\left(T^{(q)}+T^{(l)}+2h\right)}\left(e^{i2\zeta_v d} - 2e^{i\zeta_v d} + 1\right) \\ &\quad + e^{i\zeta_v\left|T^{(q)}-T^{(l)}\right|}\left(e^{i\zeta_v d} + e^{-i\zeta_v d} - 2\right) \end{aligned} \tag{A6}$$

$$\mathrm{X}_2(\zeta_v) = e^{i2\zeta_v\left(T^{(q)}+h\right)}\left(e^{i2\zeta_v d} - 2e^{i\zeta_v d} + 1\right) + 2\left(e^{i\zeta_v d} - 1\right) \tag{A7}$$

REFERENCES

1. Sheingold, L. S. and J. E. Storer, "Circumferential gap in a circular wave guide excited by a dominant circular-electric wave," *J. Appl. Phys.*, Vol. 25, No. 5, 545–552, May 1954.
2. Morita, N. and Y. Nakanishi, "Circumferential gap in a TE_{01}-mode-transmitting multimode circular waveguide," *IEEE Trans. Microwave Theory Tech.*, Vol. 16, No. 3, 183–189, Mar. 1968.
3. Park, J. K. and H. J. Eom, "Radiation from multiple circumferential slots on a conducting circular cylinder," *IEEE Trans. Antennas Propagat.*, Vol. 47, No. 2, 287–292, Feb. 1999.
4. Shin, D. H. and H. J. Eom, "Radiation from narrow circumferential slots on a conducting circular cylinder," *IEEE Trans. Antennas Propagat.*, Vol. 53, No. 6, 2081–2088, Jun. 2005.
5. Ock, J. S. and H. J. Eom, "Radiation of a Hertzian dipole in a conducting circular cylinder with narrow circumferential slots," *2006 International Symposium on Antennas and Propagation*, Singapore, Nov. 1–4, 2006.

6. Kang, M. G. and H. J. Eom, "EM penetration into narrow circumferential slots on a conducting circular cylinder," *2007 International Symposium on Antennas and Propagation*, 189–192, Japan, Aug. 20–24, 2007.
7. Park, J. K., J. N. Lee, D. H. Shin, and H. J. Eom, "A full-wave analysis of a coaxial waveguide slot bridge using the Fourier transform technique," *Journal of Electromagnetic Waves and Applications*, Vol. 20, No. 2, 143–158, 2006.
8. Hamid, A. K., "Multi-dielectric loaded axially slotted antenna on circular or elliptic cylinder," *Journal of Electromagnetic Waves and Applications*, Vol. 20, No. 9, 1259–1271, 2006.
9. Kukharchik, P. D., V. M. Serdyuk, and J. A. Titovitsky, "Diffraction of hybrid modes in a cylindrical cavity resonator by a transverse circular slot with a plane anisotropic dielectric layer," *Progress In Electromagnetics Research B*, Vol. 3, 73–94, 2008.
10. Svezhentsev, A. Y., "Mixed-potential Green's function of an axially symmetric sheet magnetic current on a circular cylindrical metal surface," *Progress In Electromagnetics Research*, PIER 60, 245–264, 2006.
11. Park, J. K. and H. J. Eom, "Fourier transform analysis of dielectric-filled edge-slot antenna," *Radio Sci.*, Vol. 32, No. 6, 2149–2154, Nov.–Dec. 1997.
12. [Online]. Available: http://www.cst.com